

Three-dimensional effects for supported excavations in clay

Richard J. Finno¹ M. ASCE, J. Tanner Blackburn² A.M. ASCE and Jill F. Roboski³ A.M.
ASCE

ABSTRACT

This paper presents the results of 159 finite element simulations conducted to define the effects of excavation geometry, i.e., length, width and depth of excavation, wall system stiffness, and factor of safety against basal heave on the 3-dimensional ground movements caused by excavation through clays. The results of the analyses are represented by the plane strain ratio, PSR, defined as the maximum movement in the center of an excavation wall computed by 3-dimensional analyses normalized by that computed by a plane strain simulation. A simple equation for PSR is presented based on excavation geometry, wall system stiffness and factor of safety against basal heave. This PSR equation reasonably represents trends in results of the 159 simulations as well as those simulations reported in literature. When the excavated length normalized by the excavated depth of an excavation wall is greater than 6, results of plane strain simulations yield the same displacements in the center of that wall as those computed by a 3-D simulation.

¹ Professor, Department of Civil and Environmental Engineering, Northwestern University, Evanston, IL 60208, r-finno@northwestern.edu

² Assistant Professor, Department of Civil Engineering, Texas A&M University, College Station, TX

³ Engineer, GeoSyntec Consultants, Chicago, IL 60601, jroboski@geosyntec.com

INTRODUCTION

Evaluating the magnitude and distribution of ground movements adjacent to an excavated wall is an important part of the design process when excavating in an urban environment. Three-dimensional effects caused by the higher stiffness at the corners of an excavation lead to smaller ground movements near the corners and larger ground movements towards the middle of the excavation wall. Another, and not necessarily universally recognized, consequence of the corner stiffening effects is the maximum movement near the center of an excavation wall may not correspond to that found from a conventional plane strain simulation of the excavation, i.e., 3-dimensional and plane strain simulations of the excavation do not yield the same movement at the center portion of the excavation, even if the movements in the center are perpendicular to the wall. While the former 3-d effect is clear in all field data reported in literature, the latter effect cannot be evaluated solely by field data.

While performance data reported in literature is inherently 3-dimensional, common semi-empirical methods to define wall movements (e.g., Clough et al. 1989) based on wall stiffness and factor of safety against basal heave are based in part on plane strain finite element simulations of excavations. It is important to recognize when one can reduce the maximum ground movement estimated with a semi-empirical method on the basis of a 3-dimensional effect. Furthermore, as inverse analysis techniques become more common in the application of the observational method to supported excavations (e.g., Finno and Calvello 2005), it is important to know when an excavation can be adequately modeled as plane strain so as to distinguish between corner stiffening effects and constitutive responses of the soil without resorting to a full 3-dimensional simulation

of the excavation.

This paper presents the results of a finite element parametric study conducted to define the effects of excavation geometry (i.e., length, width and depth of excavation), wall stiffness and factor of safety against basal heave on the 3-dimensional ground movements caused by excavation through clays. The results of the analyses are represented by the plane strain ratio, PSR, defined herein as the maximum movement in the center of an excavation wall computed by 3-dimensional analyses divided by that computed by a plane strain simulation. It is commonly practice to consider plane strain results as representative of deformations near the center of an excavation wall. Ou et al. (1996) originally defined PSR in terms of the width-to-length (B/L) ratio of the wall, and the distance from the corner.

Results of parametric studies presented herein indicate that the value of PSR is affected by (i) the ratios of the length of wall to the excavation depth (L/H_e), (ii) the plan dimensions of the excavation, L/B , with L being the side where movements are computed, (iii) the wall system stiffness ($EI/\gamma h^4$) as defined by Clough et al. (1989), and (iv) the factor of safety against basal heave. Of these factors, the L/H_e ratio was the most influential for the range of parameters considered herein.

BACKGROUND

The geometry of an excavation is described by its plan view dimensions, depth of excavation and total height of wall. This geometry has a significant effect on the ground response due to excavation. Three-dimensional responses of excavations were reported by Bono et al. (1992), Wong and Patron (1993), Ou et al. (1993;1996; 2000), Chew et al.

(1997), Lee et al. (1998), Finno and Bryson (2002) and Finno and Roboski (2005). The following observations can be made from these data regarding the movements near the corner of an excavation:

1. In all cases, the ratio of corner to center movements perpendicular to a wall, $\delta_{\text{Corner}}/\delta_{\text{Center}}$, was less than 1.0 indicating that movements decrease near the corners of the excavation due to the stiffening effects of the corners. Note that this is not the plane strain ratio defined previously herein.
2. In general, the shorter the plan dimension of the excavation wall, the smaller the movement that will be measured near the center of that excavation wall due to the stiffening effects of the corner.
3. Deeper excavations experience smaller $\delta_{\text{Corner}}/\delta_{\text{Center}}$ ratios, or higher reductions in movements near the corners of the excavation as compared to shallower excavations in similar soil conditions with similar support systems.

An empirical procedure that relates the geometry of the excavation to the distribution of $\delta_x/\delta_{\text{Center}}$ where δ_x is the lateral movement at any distance x along a wall, and, hence, the distribution of ground movements parallel to an excavation wall, has been proposed Roboski and Finno (2005). However neither the field data nor the empirical procedure provides direct information concerning whether the maximum movements can be reliably estimated on the basis of plane strain assumptions. To develop such guidelines, both 3D and 2D analyses of the same excavation must be conducted. By comparing the results of such analyses, one can define the conditions wherein the 2D plane strain results are

applicable to the actual 3D geometry and develop factors that define the stiffening effects near the corners.

A number of finite element studies have been performed to evaluate this question including those reported by Ou et al. (1993, 1996), Chew et al. (1997), Lee et al, (1998) and Lin et al. (2003). From these studies, the following observations may be drawn concerning the difference between the plane strain 2D calculation of movements near the center of the excavation wall and the 3D calculation.

1. As was seen in the field data, all studies show that smaller movements develop at the corners as compared to the center of the excavation wall. Furthermore, movements near the center of the excavation wall calculated by finite element approaches may be different in 2D plane strain analysis than in 3D.
2. For excavations with deep elevations to a rigid stratum from the excavation bottom, 2D calculation of movements near the center of the excavation wall generally over-predicted the measured field response. Results of 3D analysis more closely reflected the field response.
3. The 2D and 3D calculation of movements near the center of a “long wall” are similar for an excavation with a rigid layer immediately below the excavation bottom.
4. For smaller ratios of length of wall to height of excavation (L/H_e), the 2D analysis overestimated the amount of movement which would occur near the center of the

excavation wall, while the results of the 3D analysis better agreed with the measured movements.

In summary, both field and numerical studies show that the three-dimensional effects depend on the plan geometry and depth of excavation, support system stiffness, and depth to a rigid stratum below the excavation. However, no systematic evaluation of all these factors has been made. The following parametric study addresses these influences.

FINITE ELEMENT MODEL AND PROCEDURES

The commercially available Plaxis 3D Foundation and 2D v8.0, three-dimensional and plane strain geotechnical finite element software packages, respectively, were employed to conduct the parametric study. Structural elements were modeled with anisotropic linear and non-linear elastic elements. Soil elements are 15-node wedge elements which are created by the projection of two-dimensional, 6-node triangle elements. Variations in stratigraphy interfaces (i.e., non-horizontal) were modeled by 13-node pyramid elements and 10-node tetrahedral elements. Support structure elements consist of 3-node line elements for beams, and 6-node and 8-node plate elements for walls. Soil-structure interaction is simulated by 12-node and 16-node interface elements. Soil responses are defined by the Hardening Soil (H-S) model (Schanz et al. 1999). For more details concerning the finite element representation, see Blackburn (2005).

Parametric variables

One hundred and fifty 3D finite element analyses were made to evaluate the influence of geometric and structural parameters on horizontal soil deformation, as summarized in

Table 1. One-quarter of an excavation was represented to take advantage of symmetry, as shown in Figure 1. The primary length, L , represents the side of the wall where the lateral movement is reported, and is not necessarily the longer of the two sides (see Table 1). L varied from 20 to 160 m. The secondary length of the wall, B , varied from 10 to 160 m, such that the L/B ratio varied from 0.25 to 4. The smallest excavation modeled was 20 m x 20 m and the largest was 160 m x 80 m, such that the plan areas analyzed spanned those of typically-sized excavations in urban areas. The excavation depth, H_e , varied from 9.8 to 16.3 m such that L/H_e varied from 0.5 to 12. The side boundaries of the mesh are constrained by ‘roller’ fixities to prevent displacement in the perpendicular direction to the boundary and the bottom boundary prevents displacements both horizontally and vertically. In all cases, the mesh boundaries were located at least 120 meters from the excavation boundary. This distance was approximately seven times the maximum depth of excavation, H_e , which exceeds the minimum distance to the mesh boundary of $5H_e$, recommended by Roboski (2004). The excavation was supported by three or four levels of lateral support. The walls were ‘wished’ into place for all analyses, (i.e., installation of the wall caused no stress changes or displacements in the surrounding soil). Soil was excavated uniformly 1 m below each support level prior to adding the support.

As shown in Figure 2, two soil stratigraphies were considered to evaluate the influences of distance to a stiff layer and basal stability on three-dimensional restraining effects. The base case soil stratigraphy and support system geometry employed in this analysis corresponds to the Lurie Excavation (Finno and Roboski, 2005) in Chicago, IL, and is shown in Figure 2a. The water table is located at an elevation of 0 m. The major

difference between the stratigraphies is the depth below the excavation of a stiffer clay layer. Figure 2a represents a shallower depth, resulting in factors of safety against basal heave (Terzaghi 1943) of 1.6 to 1.8 which are larger than the values of factor of safety of 1.28 to 1.42 computed based on the stratigraphy with a greater depth to a stiff layer shown in Figure 2b.

The wall system stiffness, S , (Clough et al. 1989) is:

$$S = \frac{EI}{\gamma_w h^4} \quad (1)$$

where EI is the bending stiffness of the wall, h is the average vertical spacing of lateral support elements, and γ_w is the unit weight of water. Values of 32, 320 and 3200, were used to represent flexible, medium and stiff walls, respectively. The depth of embedment of the wall was at least 20% of the exposed height of the wall in all cases to prevent the toe of the wall from excessively deforming towards the excavation.

Soil and structural parameters

All soil layers were modeled using the H-S model. This effective stress model is formulated within the framework of elasto-plasticity. Plastic strains are calculated assuming multi-surface yield criteria. Isotropic hardening is assumed for both shear and volumetric strains. The flow rule is non-associative for frictional shear hardening and associative for the volumetric cap. The parameters used for the H-S soil model are representative of the compressible glacial clays in the Chicago area, and were obtained by

comparing computed values of lateral movements with those measured at the Ford Design Center excavation (Blackburn 2005) using inverse analysis techniques and are listed in Table 2. These parameters include the friction angle, ϕ , cohesion, c , dilation angle, ψ , the reference secant Young's modulus at the 50% stress level, E_{50}^{ref} , the reference oedometer tangent modulus, E_{oed}^{ref} , and the exponent m which relates reference moduli to the stress level dependent moduli (E representing E_{50} and E_{oed}):

$$E = E^{ref} \left(\frac{c \cot \phi - \sigma'_3}{c \cot \phi + p^{ref}} \right)^m \quad (2)$$

where p^{ref} is a reference pressure equal to 100 stress units and σ'_3 is the minor principal effective stress. Note that finite element results previously reported in literature will be compared later in this paper with results based on the H-S model and the given set of parameters to show the relative insensitivity of the PSR to the assumed soil model. A detailed description of the parameters used to model the internal bracing in 3-D is presented by Blackburn and Finno (2006). Table 3 summarizes the wall stiffness parameters. The horizontal bending stiffness is computed assuming that the wall is 20 times more flexible in the horizontal direction (the 2-direction in Table 3 indicating the direction along the length of the wall or the horizontal direction) to account for the rotations in the connections of a sheet pile wall and the lack of continuity in stiffer wall systems in this direction.

GEOMETRY, STIFFNESS AND BASE STABILITY EFFECTS

General trends

To illustrate the pattern of lateral deformations, δ , Figure 3 shows the results of 2D and 3D calculations for both the 20 m by 20 m and 80 m by 80 m excavations. The lateral deformations represent those at the end of the excavation for a vertical line located 3 m behind the center of the wall. Results are presented for excavation depths of 9.8, 13.4 and 16.3 m. The maximum movements occur slightly below the bottom of the excavated surface. Note that very little cantilever movements occur, and thus the results presented hereafter are applicable to excavations where this type of movement is minimized by installing the first level of support prior to the development of significant cantilever movements. The movements computed by the 3D analysis are less than those computed by plane strain simulations for the smaller excavations but are almost the same for the larger excavations.

Effects of excavation size and depth

The influence of excavation geometry on lateral soil displacement is evaluated by comparing the *PSR* values for several normalized geometric parameters. Figure 4a shows the relationship between *PSR* and the ratio of primary wall length to elevation depth, L/H_E , based on all cases shown in Table 2. While a variety of wall stiffness, soil stratigraphy and soil models were employed to develop these results, the general trends in the *PSR* are similar. The trends indicate that L/H_E ratios greater than 6 result in an excavation response which has a *PSR* approximately equal to 1, thus suggesting that results of plane strain and 3D analyses will yield the same maximum wall displacement in the center of the excavation. Large differences between plane strain and 3D responses are apparent when L/H_e is less than 2, implying that as the excavation gets deeper relative to its length, more restraint is provided by the sides of the excavation. Figure 4b shows

the same results plotted versus L/B ratio. When this ratio is less than or equal to 2, L/H_E must be taken into consideration for determining the PSR . Smaller values are apparent for L/B values less than 1, indicative of movement on the shorter side of the excavation. Note that there is less scatter in the $PSR-L/H_e$ plot in Figure 4a than in the $PSR-L/B$ plot in 4b suggesting that of these two geometric parameters, L/H_e is more influential in defining the PSR . The scatter in Figure 4a can be attributed to the L/B ratio, system stiffness and FS_{BH} .

Effects of wall stiffness

Figure 5 shows the $PSR-L/H_E$ relationship for each excavation depth and wall stiffness. For L/H_E values less than 2, whereas the PSR values of the medium and flexible walls increase as the excavation progresses, the stiff wall PSR values remain low (approximately 0.6), indicating additional corner restraint due to the higher wall stiffness.

Effects of Factor of Safety against Basal Heave

Figure 6 shows the relationship between PSR and L/H_E for flexible and stiff walls and different factors of safety. The trend lines plotted through the data show that for an L/H_E ratio of six or greater, the PSR value is one, regardless of stratigraphy and stability. For all wall stiffnesses, the PSR decreases with smaller L/H_E values. For flexible walls, the FS_{BH} has relatively little effect on the PSR values. In contrast, stiff walls have a greater restraining effect, and thus a smaller value of PSR when the FS_{BH} is lower.

GUIDELINES FOR ESTIMATING PSR

While Figures 4 through 6 provide guidelines for estimating PSR for the conditions shown, to quantify more generally the influences of L/H_e , L/B , S and FS_{BH} on PSR , the following equation was developed from the results of the finite element parametric study:

$$PSR = \left(1 - e^{-k C(L/H_e)}\right) + 0.05(L/B - 1) \quad (3)$$

where C is a factor that depends on the FS_{BH} and k is a factor that depends upon system stiffness. Equation 3 was found by separately evaluating the changes in PSR from a base case excavation for each main parameter. The base case represents a square excavation with a FS_{BH} approximately equal to 1.7 supported by a flexible wall with S equal to 32. In the base case, both k and C are equal to 1.

The value of k in equation 3 depends on the support system stiffness, S , and is taken as:

$$k = 1 - 0.0001(S) \quad (4)$$

This relation is illustrated in the results shown on Figure 7 where k values based on equation 2 for the computed PSR for all $L/B = 1$ data are plotted for the three system stiffness values. The trends in the computed responses are reasonably represented by equation 4.

The effects of wall stiffness on PSR as predicted via equation 3 are shown on Figure 8. An excavation depth of 13.4 m with $L/B = 1$ is shown to illustrate the following trends. Stiff walls result in lower values of PSR for a given geometry with the largest effects at

small values of L/H_e . As L/H_e gets larger, the effects of wall stiffness become less pronounced.

The value of C in equation 3 depends on the factor of safety against basal heave, FS_{BH} , and is taken as:

$$C = 1 - \{0.5 (1.8 - FS_{BH})\} \quad (5)$$

This relation is illustrated in the results shown on Figure 9 where C values based on equation 2 for all cases where the PSR was less than 0.9. The trends in the computed responses are reasonably represented by equation 5.

A comparison of the predictions made via equation 2 and results of all parametric studies presented herein and those presented in literature is made in Figure 10. In the figure, the solid line represents a base case with the k and C constants equal to 1. This corresponds to a flexible support system (where the $0.0001S$ term is negligible in equation 3) and a factor of safety against basal heave (FS_{BH}) greater than or equal to 1.8.

The dashed lines in Figure 10 represent upper and lower bounds of equation 3. The upper bound shown in Figure 10 corresponds to a base curve (k and C equal to 1) with an excavation geometry term (L/B) greater than 4. This geometry approximates plane strain conditions and, therefore, a PSR value close to unity for all L/H_e values would be expected. The lower bound curve is calculated with a combined kC constant in equation 2 equal to 0.5. A kC value equal to 0.5 reflects a range of extreme conditions that would influence the PSR , including a very stiff wall ($S=5000$) in stable material ($FS_{BH}=1.8$) to a flexible wall ($S\sim 30$) in an unstable material ($FS_{BH}=0.8$). Also, the second term in

equation 3 is assigned a value of 0.0375 for calculation of the lower bound curve. This corresponds to a low L/B ratio (0.25), which represents the case where the length of the primary wall is much shorter than the secondary wall. Large corner restraining effects would be expected for this case, thus the PSR value is reduced for all L/H_e values. In spite of different soil models and assumptions used in making the finite element analyses, the trends in the finite element results are reasonably represented by limits computed from equation 3.

In summary, the magnitude of the corner effects depends on the geometry of the excavation, the stiffness of the support system, and the factor of safety against basal heave. In general, greater corner effects are observed for relatively deep excavations, as evidenced by small L/H_e values, on the shorter of the two walls, as evidenced by L/B values less than 1, for stiff walls and for lower factors of safety against basal heave. Conversely, when L/H_e is larger than 6, plane strain and 3-D analyses yield the same maximum movements in the center of the excavation for the range of conditions analyzed herein.

COMPUTED HORIZONTAL DISPLACEMENTS

Figure 11 compares the computed horizontal soil deformation distributions for the 20m x 20m and 80m x 80m excavations at each excavation depth. The horizontal distributions correspond to the displacement at elev. -7.0 m, which is the approximate elevation of the maximum horizontal displacement. For each excavation geometry, the maximum displacement decreases with increasing wall stiffness, however the distribution shapes do

not differ significantly for each wall stiffness. The shape of the distributions differs between the excavation geometries, as the zone of ‘plane-strain’ deformation is much greater for the 80 m excavation. Also shown is the distribution of the lateral movements as computed by a complementary error function defined as (Finno and Roboski 2005; Roboski and Finno 2006):

$$\delta(x) = \delta_{\max} \left(1 - \frac{1}{2} * \operatorname{erfc} \left(\frac{2.8(x + L [0.015 + 0.035 \ln \frac{H_e}{L}])}{0.5L - L [0.015 + 0.035 \ln \frac{H_e}{L}]} \right) \right) \quad (6)$$

Use of this equation requires only geometry and an estimate of the maximum movement. As can be seen on Figure 11, the complementary error function better matches the distributions for the flexible wall than for the stiff wall, although reasonable agreement is seen in all cases. Equation (6) was derived based on the observations at an excavation with a flexible wall. It has been shown to provide reasonable agreement for movements reported in literature for stiffer walls (Roboski and Finno 2006), however, it is not altogether unexpected that better agreement is found for flexible walls.

CONCLUSIONS

Based on the results of the finite element parametric studies presented herein, the following conclusions can be drawn concerning differences between displacements computed by plane strain and 3D analyses of supported excavations in clays:

1. The plane strain ratio, PSR , defined herein as the maximum lateral movement behind a wall found from the results of a 3D simulation normalized by that from a plane strain simulation depends on geometry expressed as L/H_e and L/B ratios, wall system stiffness and factor of safety against basal heave, as expressed in equation 3.
2. When L/H_e is greater than 6, the PSR is equal to one and results of plane strain simulations yield the same displacements in the center of an excavation as those computed by a 3-D simulation.
3. All else being equal, smaller values of L/B produce lower PSR than higher values.
4. All else being equal, stiff wall systems produce lower PSR than flexible wall systems.
5. All else being equal, excavations with lower factors of safety against basal heave, FS_{BH} produce lower PSR than excavations with higher FS_{BH} .

ACKNOWLEDGMENTS

Financial support for this work was provided by National Science Foundation grant CMS-0219123 and the Infrastructure Technology Institute (ITI) of Northwestern University. The support of Dr. Richard Fragaszy, program director at NSF, and Mr. David Schulz, ITI's director, is greatly appreciated.

REFERENCES

Blackburn, J.T. (2005). Automated remote sensing and three-dimensional analysis of internally braced excavations. PhD dissertation, Northwestern University, Evanston, IL.

Blackburn, J.T. and Finno, R.J. (2006). Representing internal bracing systems in 3-D models of deep excavations, Proceedings, GeoCongress 2006, Geotechnical Engineering in the Information Technology Age, ASCE, Atlanta GA. In press.

Bono, N.A., Liu, T.K., and Soydemir, C. 1992. Performance of an Internally Braced Slurry-Diaphragm Wall for Excavation Support. *In Slurry Walls: Design, Construction, and Quality Control*, ASTM STP 1129, Edited by David B. Paul, Richard G. Davidson, and Nicholas J. Cavalli. ASTM, Philadelphia. pp. 169-190.

Chew, S. H., Yong, K. Y., and Lim, A. Y. K., 1997. "Three-dimensional finite element analysis of a strutted excavation," *Computer Methods and Advances in Geomechanics*, Yuan (editor), Balkema, Rotterdam.

Clough, G. W., Smith, E. M., and Sweeney, B. P. 1989. Movement Control of Excavation Support Systems by Iterative Design. *In Current Principles and Practices, Foundation Engineering Congress*, Vol. 2. ASCE, pp. 869-884.

Finno, R. J., and Bryson, L. S. 2002. Response of a building adjacent to stiff excavation support system in soft clay. *Journal on the Performance of Constructed Facilities*, ASCE, 16(1): 10-20.

Finno R.J., Bryson L.S. and Calvello M. (2002). Performance of a stiff support system in soft clay. *Journal of Geotechnical and Geoenvironmental Engineering*, ASCE, Vol. 128, No. 8, p. 660-671.

Finno, R.J. and Calvello, M., (2005). Supported Excavations: the Observational Method and Inverse Modeling, *Journal of Geotechnical and Geoenvironmental Engineering*, ASCE, Vol. 131, No. 7, 826-836.

Finno, R. J., and Roboski, J. F. 2005. Three-dimensional response of a tied-back excavation through clay. *Journal of Geotechnical and Geoenvironmental Engineering*, ASCE. 131(3): 273-282.

Lee, F. H., Yong, K. Y., Quan, K. C., and Chee, K. T. 1998. Effect of Corners in Struttred Excavations: Field Monitoring and Case Histories. *J. Geotech. Engrg.*, ASCE, 124(4), 339-349.

Lin, D. G., Chung, T. C., and Phien-wej, N. 2003. Quantitative evaluation of corner effect on deformation behavior of multi-struttred deep excavation in Bangkok subsoil. *Geotechnical Engineering*, 34(1), 41-57.

Ou, C. Y., and Chiou, D. C. 1993. Three-dimensional finite element analysis of deep excavation. *Proc., 11th Southeast Asian Geotechnical Conf.*, The Institute of Engineers, Malaysia, Kuala Lumpur, Malaysia, 769-774.

Ou, C. Y., Chiou, D. C., and Wu, T. S. 1996. Three-dimensional finite element analysis of deep excavations. *J. Geotech. Engrg.*, ASCE, 122(5), 473-483.

Ou, C.Y., Shiau, B.Y., and Wang, I. W. (2000a). "Three-dimensional deformation behavior of the Taipei National Enterprise Center (TNEC) excavation case history," *Canadian Geotechnical Journal*, 37, 438-448.

Ou, C.Y., Liao, J.T., and Cheng, W.L. (2000b). Building response and ground movements induced by a deep excavation. *Geotechnique*. 50(3): 209-220.

Roboski, J.F. (2004). Three-dimensional Performance and Analyses of Deep Excavations. PhD dissertation, Northwestern University, Evanston, IL.

Roboski, J.F. and Finno, R.J., (2006). Distributions of Ground Movements Parallel to Deep Excavations, *Canadian Geotechnical Journal*. in press.

Schanz T., Vermeer P.A. and Bonnier P.G. (1999). The Hardening Soil model - formulation and verification. Proceedings Plaxis Symposium "Beyond 2000 in Computational Geotechnics", Amsterdam, Balkema, p. 281-296.

Terzaghi, K. (1943). 1943. Theoretical Soil Mechanics. John Wiley and Sons, New York.

Wong, L. W. and Patron, B. C. 1993. Settlements induced by deep excavations in Taipei, Eleventh Southeast Asian Geotechnical Conference, Singapore.

List of Tables

Table 1. Summary of 3D finite element analyses for parametric study

Table 2. Hardening soil parameters used in parametric study

Table 3. Wall stiffness parameters

List of Figures

Figure 1. Finite element mesh

Figure 2. Subsurface conditions for parametric studies

Figure 3. Lateral soil movements behind the wall: plane strain vs 3D

Figure 4. Effect of plan dimensions and excavation depth on *PSR*

Figure 5. Effects of support system stiffness

Figure 6. Effects of basal stability

Figure 7. Parameter *k* as a function of support system stiffness

Figure 8. Effects of support system stiffness for $L/B = 1$

Figure 9. Parameter *C* as a function of basal stability

Figure 10. Comparison between published data and results of parametric study

Figure 11. Computed and empirically-derived lateral movements along wall

Table 1. Summary of 3D finite element analyses for parametric study

Stratigraphy (see Figure 2)	Height of cut, H_e (m) / FS_{BH}	Primary length of cut, L (m)	Secondary length of cut, B (m)
A	9.8/1.7, 13.4/1.68, 16.3/1.8	20	20, 40, 80
		40	20, 40, 80
		80	20, 40, 80, 160 ¹
		160	80 ¹
B	9.8/1.63, 13.4/1.42, 16.3/1.28	20	20, 40
		40	20, 40, 80
		80	40, 80

Notes: ¹ analyzed for H_e equal to 9.8 m only.

System stiffnesses of 32, 320 and 3200 were considered for each of the above 50 cases.

Table 2. Hardening soil parameters used in parametric study

Parameter	Sand	Soft clay	Medium clay	Stiff clay
E_{50}^{ref} (kPa)	7,185	421	1,284	17,723
$E_{\text{oed}}^{\text{ref}}$ (kPa)	7,185	295	884	12,406
c^{ref} (kPa)	1	1	1	1
ϕ (°)	37	24	26	32
Ψ (°)	5	0	0	0
m	0.5	0.8	0.85	0.85

Table 3. Wall stiffness parameters

Parameter	Flexible wall	Medium wall	Stiff wall
Plane strain FE parameters			
System stiffness, S	32	320	3200
Bending stiffness, EI (kN-m ² /m)	50,400	504,000	5,040,000
Axial stiffness, EA (kN/m)	3,427,000	34,270,000	342,700,000
Element thickness (m)	0.42	0.42	0.42
Poisson's ratio	0	0	0
Three-dimensional FE parameters			
Young's modulus, E ₁ (kPa)	8,160,000	81,600,000	816,000,000
Young's modulus, E ₂ (kPa)	408,000	4,080,000	40,800,000
Young's modulus, E ₃ (kPa)	200,000,000	2,000,000,000	20,000,000,000
Shear Modulus, G ₁₂ (kPa)	408,000	4,080,000	40,800,000
Shear Modulus, G ₁₃ (kPa)	400,000	4,000,000	40,000,000
Shear Modulus, G ₂₃ (kPa)	1,330,000	13,300,000	133,000,000
Poisson's ratio	0	0	0
Element thickness (m)	0.42	0.42	0.42

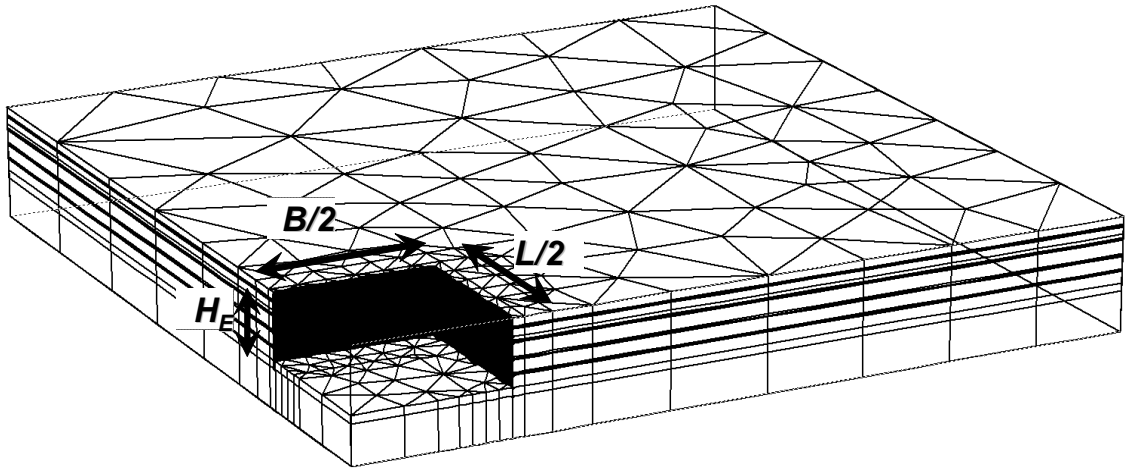


Figure 1. Finite element mesh

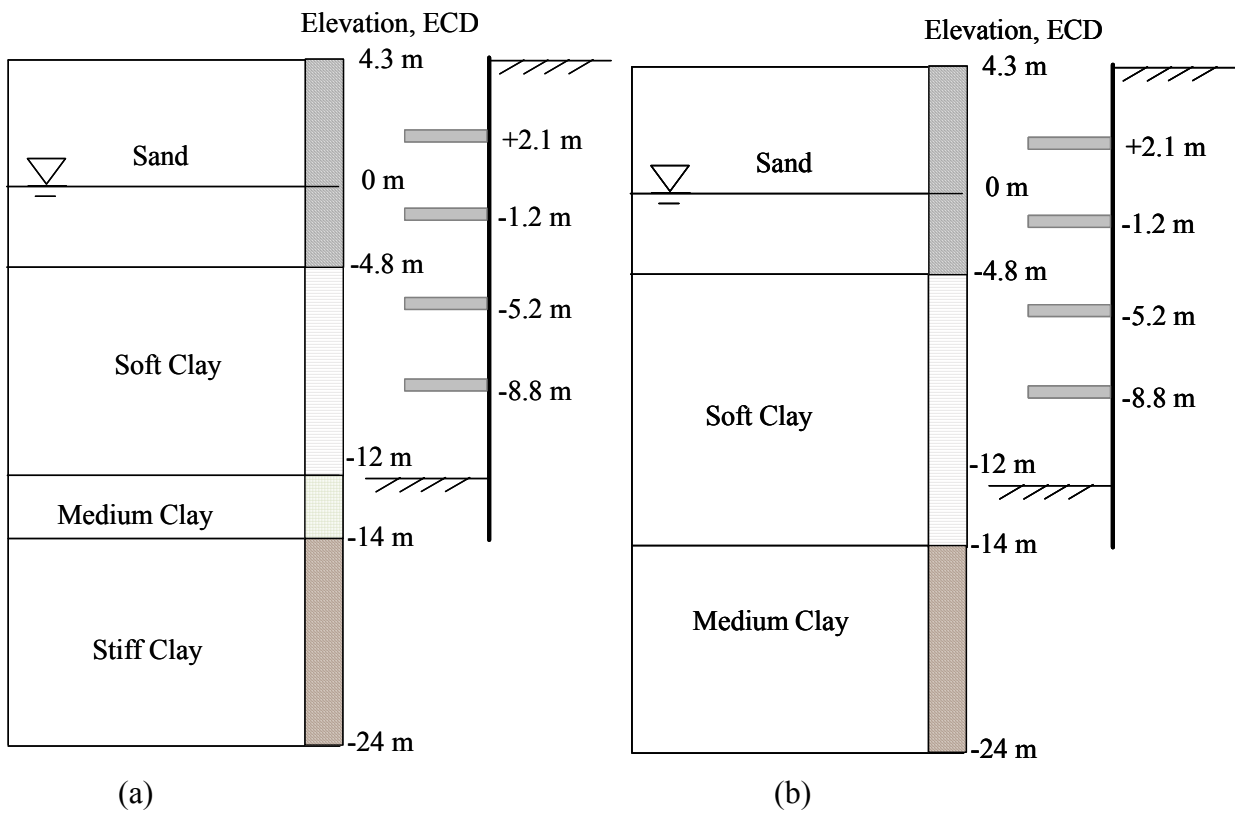


Figure 2. Subsurface conditions for parametric studies

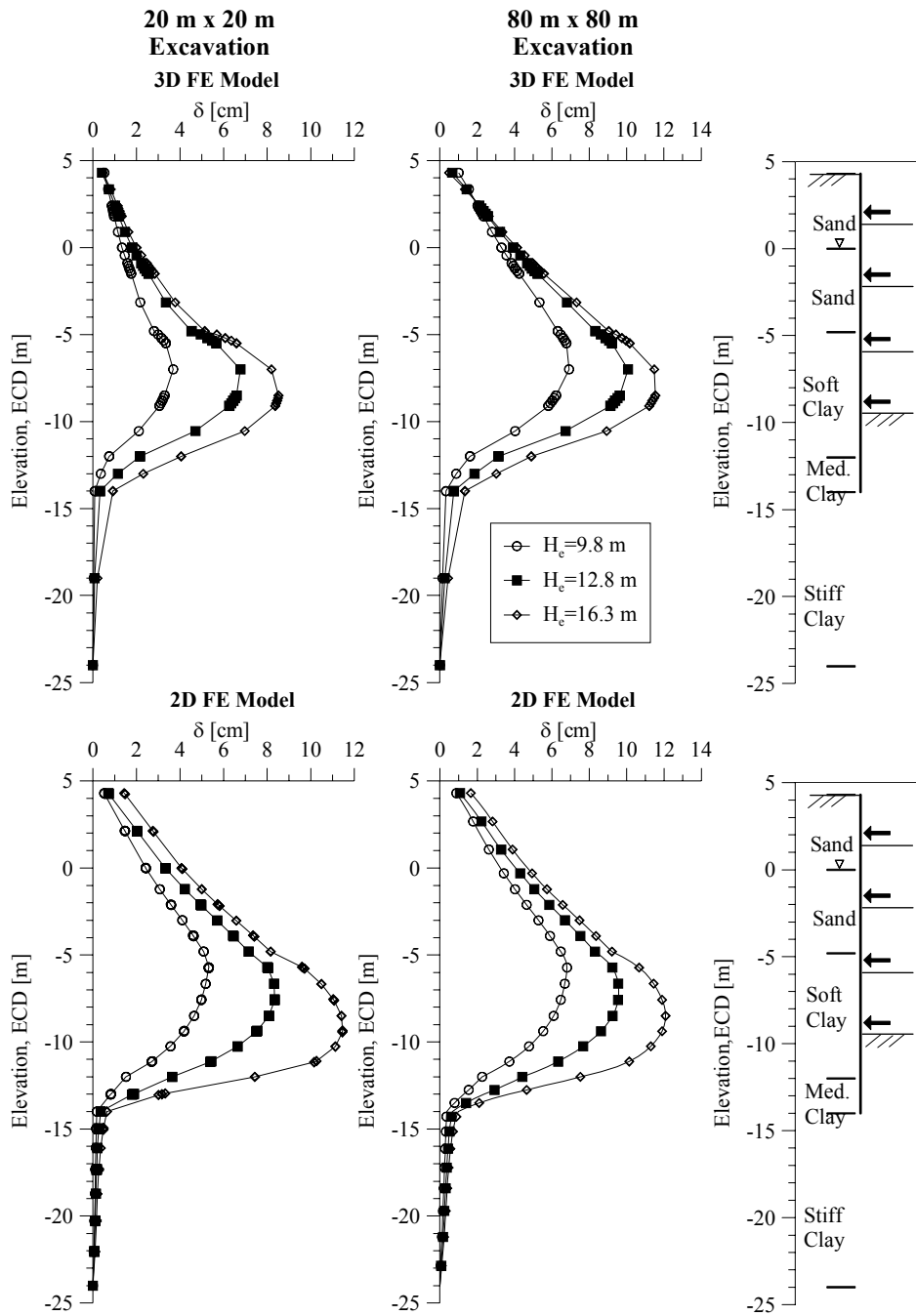


Figure 3. Lateral soil movements behind wall: plane strain versus 3D

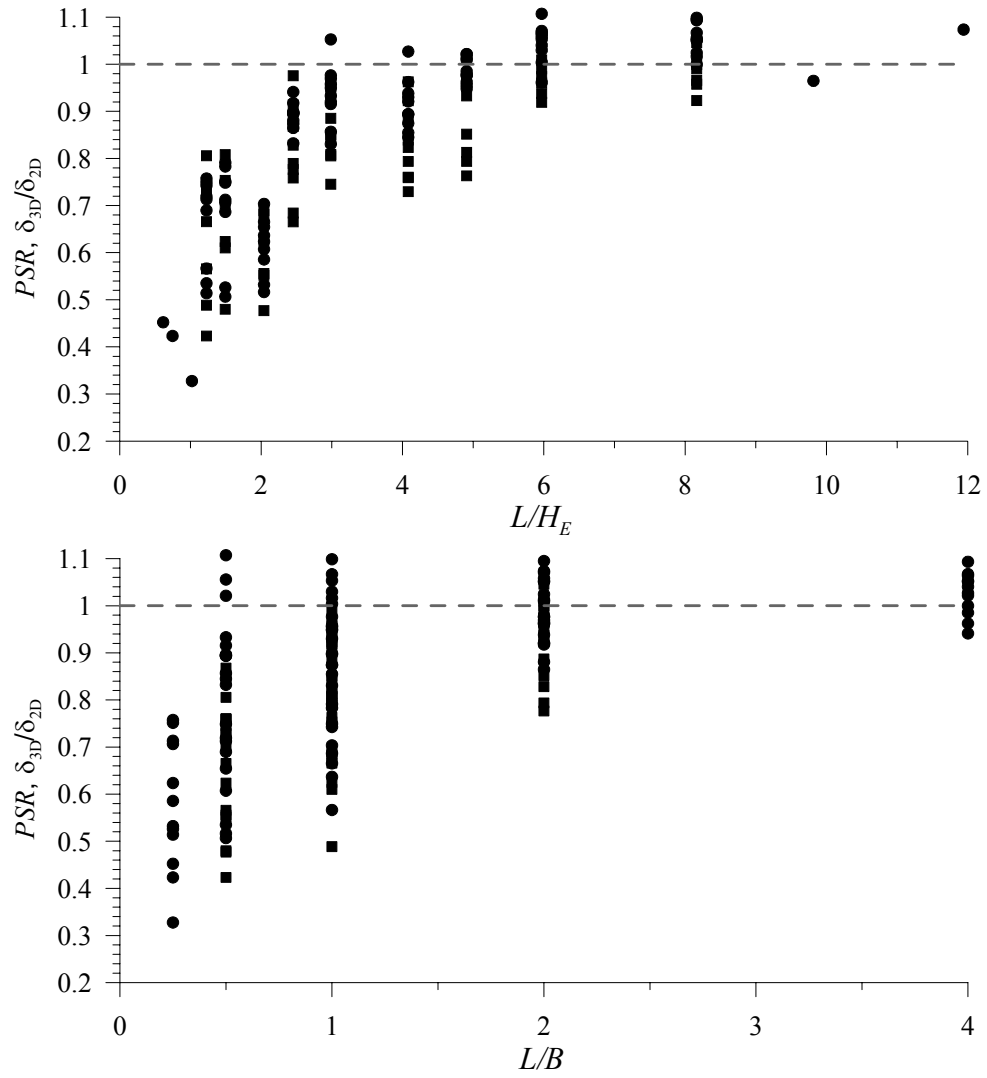


Figure 4. Effects of plan dimensions and depth of excavation on PSR

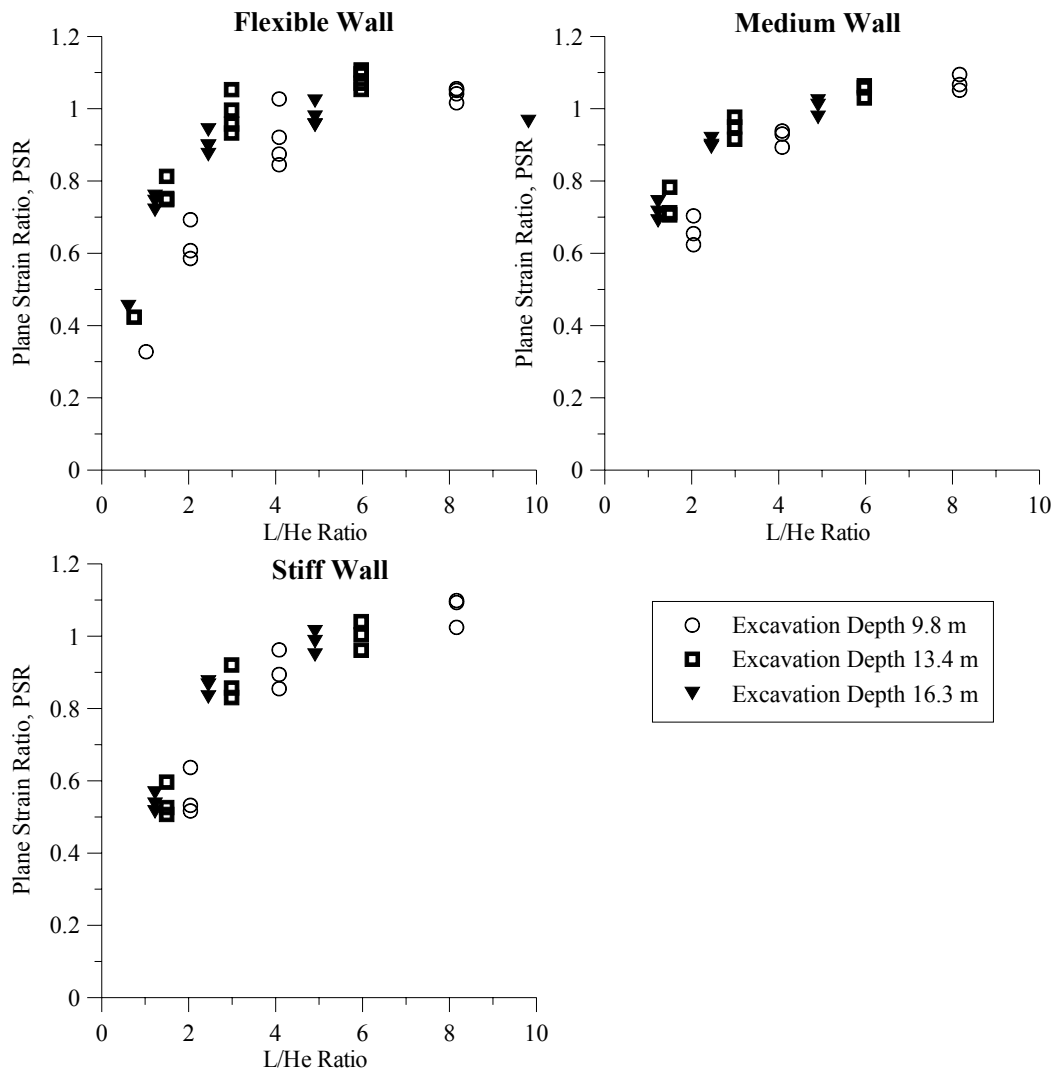


Figure 5. Effects of support system stiffness

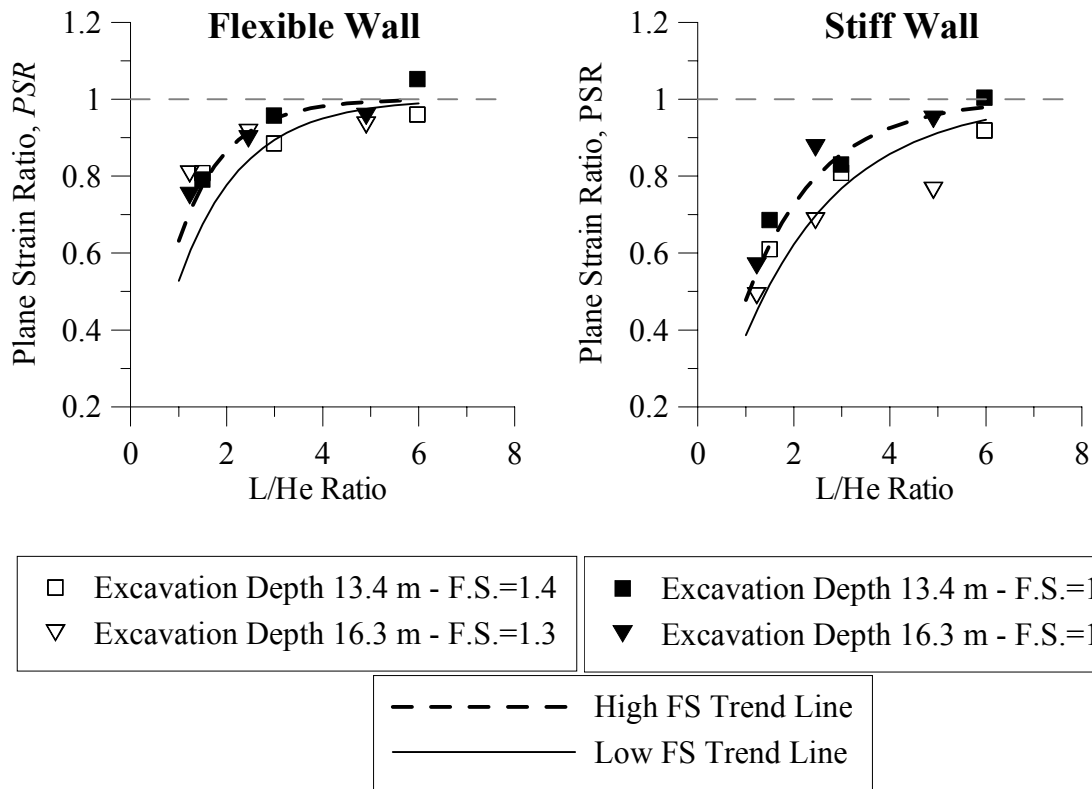


Figure 6. Effects of basal stability

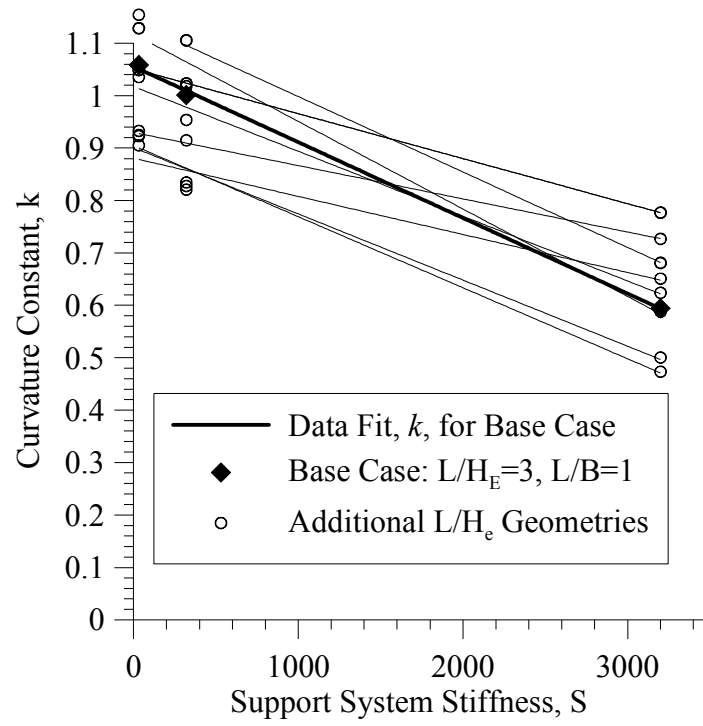
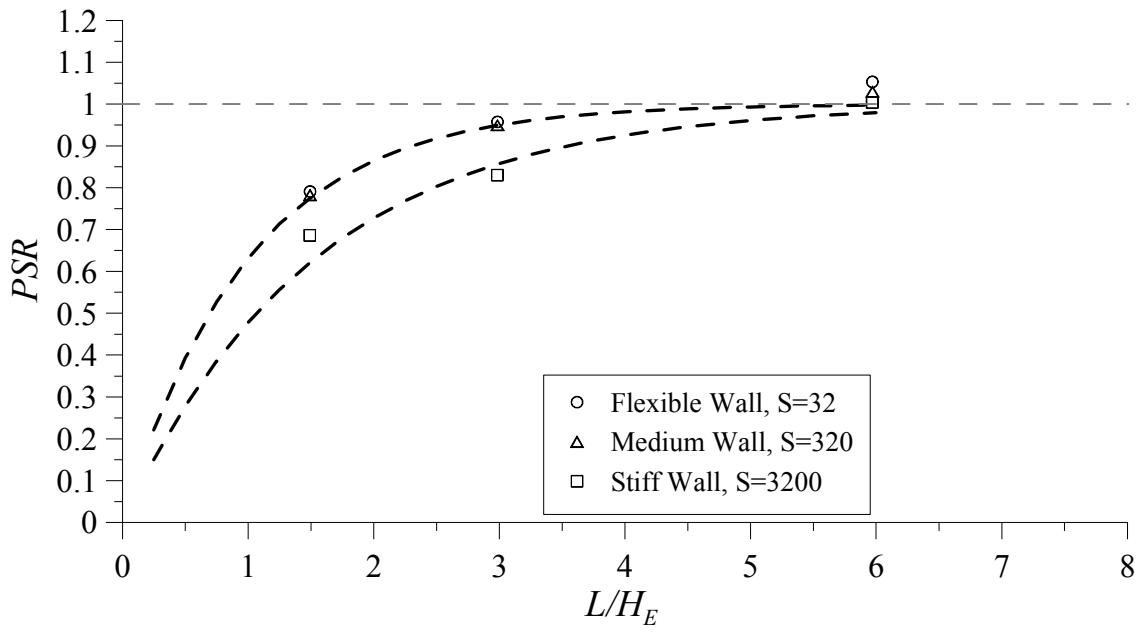


Figure 7. Parameter k as a function of support system stiffness



Note: Excavation Depth 13.4m, L/B=1

Figure 8. Effects of support system stiffness for L/B = 1

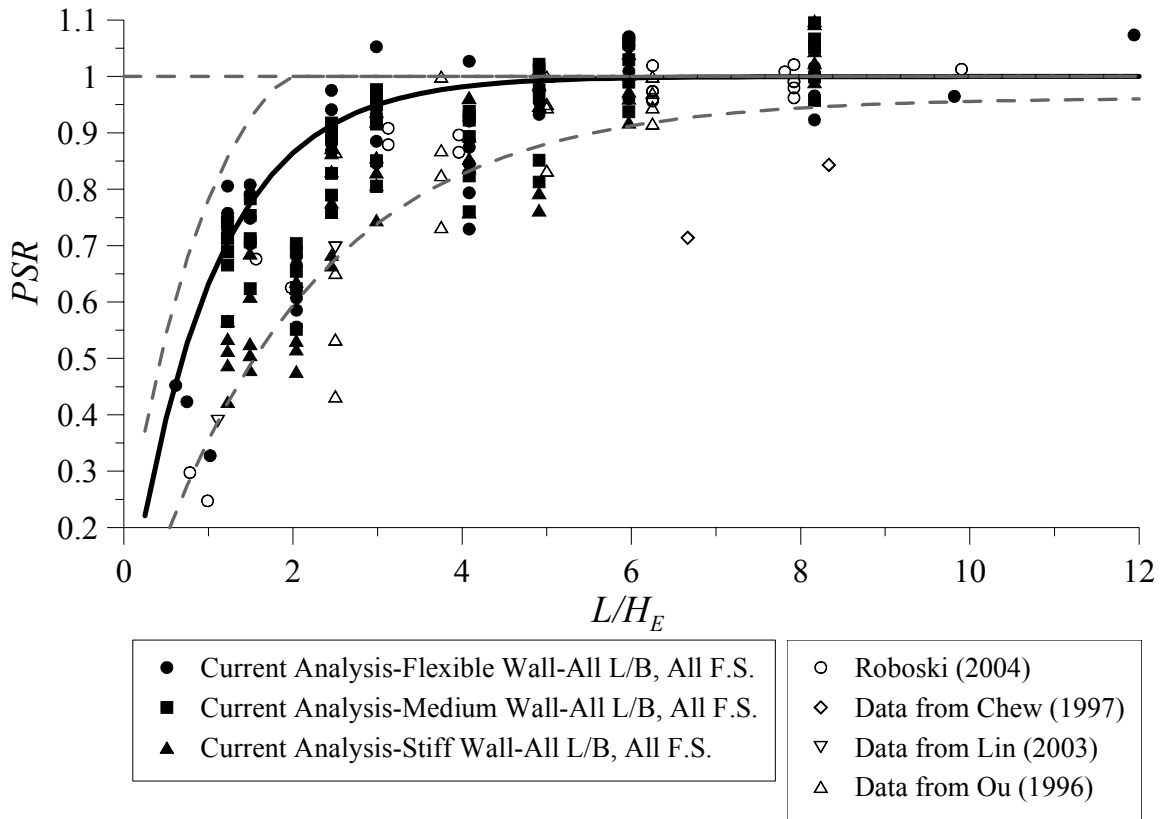


Figure 10. Comparison between published data and results of parametric study

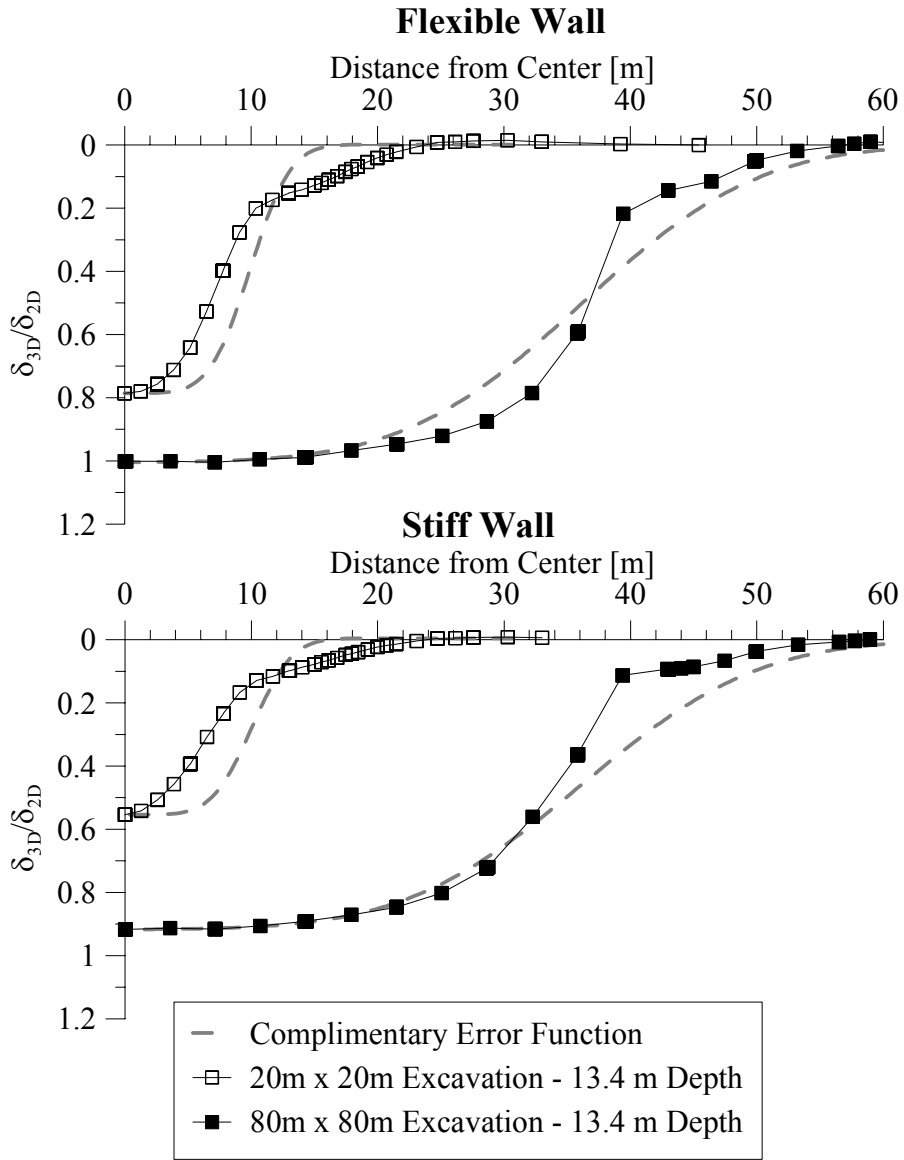


Figure 11. Computed and empirically-derived lateral movements along wall